PHYSICAL REVIEW A VOLUME 50, NUMBER 4 OCTOBER 1994

Electron-impact collision strengths for neutral fluorine

Kiran S. Baliyan* and A. K. Bhatia
Laboratory for Astronomy and Solar Physics, NASA Goddard Space Flight Center, Greenbelt, Maryland 20771

(Received 10 February 1994)

Configuration-interaction wave functions are constructed for the lowest 11 atomic target states of neutral fluorine. These wave functions are used to calculate target-state energies and absorption oscillator strengths for the dipole-allowed transitions. In general, a good agreement is found between the length and velocity forms of f values. However, f values for some transitions show significant discrepancies between these two forms. All these target states are retained in the R-matrix basis function and the $(N+1)$-electron collision wave functions are expanded in terms of these basis functions. The calculations are performed for the electron-impact excitation collision strengths for all transitions between these states using the R-matrix method. In the low-partial-wave region (total angular momentum $L \le 12$) the full exchange R-matrix method is employed while a no-exchange R-matrix method is used for the calculations in the partial-wave region with $13 \le L \le 40$. The effect of this procedure is most evident in the case of dipole-forbidden transitions for which collision strengths increase by about 10–60% due to the contribution from higher partial waves. Beyond this value of the total angular momentum, the Burgess sum rule is applied to determine the higher partial-wave contribution to the total collision strengths for dipole-allowed transitions. The collision strengths are obtained for a wide range of incident electron energy from the first excitation threshold to 3.0 Ry. The calculations are performed in the LS-coupling scheme.

PACS number(s): 32.70.Cs, 34.80.Dp

I. INTRODUCTION

The ark spectrum of neutral fluorine was first investigated by Liden [1] who observed two emission lines at 680.709 and 682.581 Å above the first ionization threshold [$\mathrm{F}^+(2s^22p^4\,{}^3P)$] apart from many other lines. Huffman, Larrabee, and Tanaka [2] studied the absorption spectrum which was analyzed later by Palenius [3,4]. The lines of the ions of fluorine isoelectronic sequence are frequently observed in the laboratory and astrophysical plasmas [5–7]. There exists plenty of atomic data on these ions (see, for example, Mohan and Hibbert [8] and references therein). The neutral system, atomic fluorine, however, has not attracted the attention of atomic physicists. Nevertheless, the atomic data on this atom are of considerable importance, academically as well as for their possible applications in the astrophysical study of cool stars and cosmic rays. For these reasons, we decided to study neutral fluorine in some detail.

We describe target states of neutral fluorine by the configuration-interaction wave functions. The lowest 11 target states are used in the scattering calculation. These states are constructed using six orthogonal atomic orbitals: 1s, 2s, 2p, 3s, 3p, and 3d. Absorption oscillator strengths are calculated for all the transitions between these states in the length and velocity forms of the dipole operator. The electron-impact excitation data (collision strengths) are calculated for all the transitions in the LS coupling using the R-matrix [9] method. For lower partial waves with total angular momentum up to $L=12$, the full exchange R-matrix method is used as implemented in the RMATRX [10] program. Beyond this value of angular momentum, exchange effects are found to be negligible and therefore the no-exchange program of Burke, Burke and Scott [11] is used for the total angular momentum range $12 \le L \le 40$. At this value of L, collision strengths for all the transitions are converged except for the dipole-allowed transitions, which converge rather slowly. The Burgess sum rule [12] is applied to determine the higher-partial-wave contribution for these transitions.

In the next section we give a summary of the method used and other details of the calculation. In Sec. III, we present our results in the form of oscillator strengths and collision strengths. Section IV concludes the present calculation with some comments on the accuracy of these calculations.

II. CALCULATIONS

A. Target-state wave functions

We consider the lowest $2s^22p^5\,{}^2P^o$; $2s^22p^4({}^3P)3s\,{}^4P$, ${}^2P$; $2s^22p^4({}^3P)3p\,{}^4P^o$, ${}^4D^o$, ${}^2D^o$, ${}^2S^o$, ${}^4S^o$, ${}^2P^o$; $2s^22p^4({}^1D)3s\,{}^2D$ and $2s^22p^4({}^3P)3d\,{}^4D$ target states in our present LS-coupling calculation. There are several other $2p^43l$ states which fall above 1.4 Ry energy and have not been retained in the calculation in order to keep the size of the calculation manageable. The configuration-interaction (CI) wave functions for the lowest 11 target

---

*Present address: THE-PH, Physical Research Laboratory, Navarangpura, Ahmedabad 380 009, India.

states are expanded as linear combination of the configuration-state functions ϕ's,

$$\Phi_j(LS)=\sum_{i=1}^{m} a_{ij}\phi_i(\alpha_i LS) \ . \tag{1}$$

These configurations are the eigenfunctions of the total orbital and spin angular momenta (L and S) and are constructed from one-electron atomic orbitals. The radial functions of these orbitals are expressed as a sum of normalized Slater-type orbitals:

$$P_{nl}(r)=\sum_{i=1}^{k} c_i r^{p_i}\exp(-\zeta_i r) \ , \tag{2}$$

where the parameters c_i, p_i, and ζ_i are given in Table I. These parameters for 1s, 2s, and 2p atomic orbitals are taken from the tables by Clementi and Roetti [13] given for the ground state $^2P^o$ of the neutral fluorine. The CIV3 program written by Hibbert [14] was used both to optimize the rest of the parameters defining the atomic orbitals in Eq. (2) and to determine the mixing coefficients in Eq. (1). The 3s orbital radial functions were obtained by minimizing the $2s^22p^43s\ ^2P$ state energy. The average of the energies of the $2s^22p^43p\ ^2P^o$ and $2s^22p^43p\ ^4P^o$ states was used to optimize 3p orbital radial functions. This procedure gave lower energies and reasonable separation between these two target states. Finally, the 3d orbital parameters were obtained by varying its coefficients and exponents and optimizing the energy of the $2s^22p^43d\ ^4D$ state. The set of configurations constructed from these orbitals and used in the present calculation to represent the 11 target states is given in Table II. The calculated values of the target-state energies are tabulated, along with the observed [15] ones, in Table III. We find that the calculated values of the target states differ from the observed values by about 5–10 %. This is mainly due to the limited amount of configuration interaction included and the use of the common set of atomic orbitals in representing the 11 target states retained in this calculation. However, it should be noted that the 3s orbital in $2s^22p^43s\ ^4P$ is quite different from the one appropriate for the $2s^22p^43s\ ^2P$ state. Similar is the case with the 3p orbital for the $2s^22p^43p\ ^4P^o$ and $2s^22p^43p\ ^4D^o$ states. The orthogonality condition forbids the use of separate orbitals for these states. However, correlation orbitals could have been used to make up for this deficiency. But a larger set of orbitals, including the correlation orbitals, and full configuration interaction would result in a very lengthy and more involved computation and, at the same time, will introduce unphysical pseudoresonances in the calculation. In order to enable a direct comparison with experiment we have adopted the observed excitation thresholds in our collision calculations.

TABLE I. The values of parameters of the atomic orbitals for neutral fluorine.

Orbital	Coefficient	Power of r	Exponent
3s	1.568 97	1	0.529 23
	−10.223 75	2	1.550 97
	10.414 91	3	2.224 65
3p	0.074 53	2	0.333 53
	0.000 82	3	3.157 04
	−4.266 45	3	3.188 61
3d	0.010 05	3	0.343 87
	0.000 25	3	0.900 73

TABLE II. The configurations used to represent target states of fluorine.

Even parity	Odd parity
$2s^22p^43s$	$2s^22p^5$
$2s2p^6$	$2s^22p^43p$
$2s2p^53p$	$2s^22p^33p^2$
$2s^22p^43d$	$2s^22p^33s^2$
$2s2p^43s^2$	$2s^22p^33d^2$
$2s2p^43p^2$	$2s^22p^23s^23p$
$2s2p^43d^2$	$2s^22p^23p3d^2$
$2s2p^43s3d$	$2s^22p^33s3d$
$2s^22p^23s3p^2$	$2s2p^53s$
$2s^22p^33s3p$	$2s2p^53d$
$2s^22p^33p3d$	$2s2p^43s3p$
$2s^22p^23p^23d$	$2s2p^43p3d$
$2s^22p^23s^23d$	

B. Collision wave functions

The total ($N+1$)-electron wave functions describing the collision are expanded in the R-matrix internal region ($r<a$, where a is the radius of internal region) in terms of the following basis functions:

$$\psi_k=\mathcal{A}\sum_{ij} c_{ijk}\bar{\phi}_i(x_1,x_2,\ldots,x_N;\hat{\mathbf{r}}_{N+1},\sigma_{N+1})u_{ij}(r_{N+1}) + \sum_j d_{jk}\phi_j(x_1,\ldots,x_{N+1}) \ , \tag{3}$$

where $\mathcal{A}$ is the antisymmetrization operator, $\bar{\phi}_i$ are channel functions formed by coupling the target states Φ_i to the orbital and spin angular momenta of the scattering channel, u_{ij} are the continuum basis orbitals, and ϕ_j are the ($N+1$)-electron bound configurations which account

TABLE III. Calculated and observed target-state energies for fluorine relative to the ground state.

Key	Target state	Energy (Ry) Calculated	Observed[a]
1	$2s^22p^5\ ^2P^o$	0.0	0.0
2	$2s^22p^4(^3P)3s\ ^4P^e$	1.009 28	0.933 76
3	$2s^22p^4(^3P)3s\ ^2P^e$	1.033 02	0.954 45
4	$2s^22p^4(^3P)3p\ ^4P^o$	1.160 49	1.056 12
5	$2s^22p^4(^3P)3p\ ^4D^o$	1.169 62	1.066 58
6	$2s^22p^4(^3P)3p\ ^2D^o$	1.175 88	1.071 85
7	$2s^22p^4(^3P)3p\ ^2S^o$	1.181 19	1.078 07
8	$2s^22p^4(^3P)3p\ ^4S^o$	1.181 22	1.078 27
9	$2s^22p^4(^3P)3p\ ^2P^o$	1.195 92	1.083 35
10	$2s^22p^4(^1D)3s\ ^2D^e$	1.202 53	1.128 37
11	$2s^22p^4(^3P)3d\ ^4D^e$	1.229 56	1.166 27

[a] Weise and Martin [15].

both for the short-range correlation effects and also make some allowance for the omitted channels in the first expansion. They also ensure that the orthogonality conditions imposed on the u_{ij} and described below do not impose any restriction on the total wave function. The continuum orbitals u_{ij} in (3) are solutions of the radial differential equation

$$\left[\frac{d^2}{dr^2}-\frac{l_i(l_i+1)}{r^2}+V(r)+k_i^2\right]u_{ij}(r)=\sum_k \lambda_{ijk}P_{kl_i}(r) , \tag{4}$$

satisfying the boundary conditions

$$u_{ij}(0)=0 \tag{5}$$

and

$$\left.\frac{a}{u_{ij}}\frac{du_{ij}}{dr}\right|_{r=a}=b , \tag{6}$$

where $V(r)$ is the zero-order potential representing the static charge distribution of the atom, a is the radius of the sphere defining the internal region, and b is a constant, taken here as zero. The internal region radius a is chosen so that the amplitudes of the radial orbitals become negligible at the boundary of the internal region, i.e., $P_{nl}(a)<0.001$. This assures that beyond this region exchange effects are negligible and the direct interaction reaches its asymptotic form.

The R-matrix calculations in the internal region are carried out using the RMATRX [10] code. We retain 25 continuum orbitals in each channel, which are sufficient to give convergence for all energies and angular momenta considered here. The ϕ_j are constructed automatically by requiring that a minimum of two electrons are in the 1*s* and 2*s* shells, and three electrons are in 2*p* shell. The maximum number of electrons allowed in these and the 3*s*, 3*p*, and 3*d* shells are limited to 2, 2, 6, 2, 1, and 1, respectively. The maximum number of bound terms and coupled channels are 48 and 19, respectively. The R-matrix internal region radius is taken as $34.0a_0$. The calculation is performed for all partial waves with total angular momentum $L \leq 12$.

In practice, a large number of partial waves are required to obtain converged results for all the transitions. It would have been excessively expensive to use the full exchange R-matrix method for such a large number of partial waves. We therefore used the no-exchange R-matrix method [16] implemented in the RMATRX-NX [11] program for all partial waves with total angular momenta $13 \leq L \leq 40$. This program runs considerably faster than the full R-matrix program mainly for the two reasons. First, the quadratically integrable functions ϕ_j in Eq. (3) do not contribute, since these are constructed from the bound orbitals with maximum angular momentum $l=2$. Second, the calculation of exchange terms is dropped by definition.

In the asymptotic region, exchange effects have become negligible and the quadratically integrable functions, involving the bound orbitals, have died away; hence the asymptotic equations for the full exchange program and those for the no-exchange program are identical. Therefore, the calculations in the outer region are performed using the common set of programs. We have used asymptotic package VPM [17] to obtain collision strengths in both the cases. This program solves coupled differential equations using the variable phase method. The details of the programs and calculation procedure are given by Berrington *et al.* [18].

III. RESULTS

A. Oscillator strengths

The configuration-interaction wave functions for neutral fluorine generated in the earlier section are used to calculate absorption oscillator strengths in the dipole length and velocity forms using the CIV3 code. It should be noted that a good agreement between the f values calculated in these two forms is a necessary condition for the good quality of atomic wave functions. The f values calculated in the present work are reported in Table IV. In general, a limited amount of agreement is seen between the results obtained using the two forms. The relatively large differences between length and velocity forms of the oscillator strengths shown by some of the transitions considered here refer to the fact that not enough configuration interaction has been included, apart from the factor that a common set of atomic orbitals is used to represent all the target states. However, the disparity of a factor of 9 between the f values obtained using the two forms of dipole operator for the transition $3s\ ^2D^e$–$3p\ ^2D^o$ is due largely to the cancellation effects in the dipole matrix elements—a characteristic of the small oscillator strengths. It is understood that the velocity form, which emphasizes the short-range nature of the wave function, is very sensitive to the configuration interaction. The length form, which signifies the asymptotic region, is expected to be more accurate. Therefore, we believe that the target wave functions constructed here and used in the collision calculations are of reasonably good quality.

TABLE IV. The oscillator strengths for the transition in neutral fluorine.

Transition	Oscillator strength	
i-f	L	V
$2s^22p^5\ ^2P^o$–$2s^22p^43s\ ^2P^e$	8.8083[−2][a]	9.5368[−2]
$2s^22p^43s\ ^2P^e$–$2s^22p^43p\ ^2P^o$	4.2715[−1]	2.0533[−1]
$2s^22p^5\ ^2P^o$–$2s^22p^43s\ ^2D^e$	4.6566[−2]	4.5069[−2]
$2s^22p^43s\ ^2D^e$–$2s^22p^43p\ ^2P^o$	2.4470[−3]	8.5719[−4]
$2s^22p^5\ ^2P^o$–$2s^22p^43s\ ^2S^e$	1.5268[−2]	1.7432[−2]
$2s^22p^43p\ ^2P^o$–$2s^22p^43s\ ^2S^e$	1.3490[−2]	2.0683[−3]
$2s^22p^43s\ ^4P^e$–$2s^22p^43p\ ^4P^o$	4.3744[−1]	1.6631[−1]
$2s^22p^43s\ ^4P^e$–$2s^22p^43p\ ^4S^o$	1.4645[−1]	5.3922[−2]
$2s^22p^43p\ ^4P^o$–$2s^22p^43s\ ^4D^e$	9.9547[−1]	6.5772[−1]
$2s^22p^43p\ ^4P^o$–$2s^22p^43d\ ^4D^e$	1.5686[−2]	1.2536[−2]
$2s^22p^43p\ ^4D^o$–$2s^22p^43d\ ^4D^e$	1.8234[−1]	1.3198[−1]
$2s^22p^43s\ ^2P^e$–$2s^22p^43p\ ^2D^o$	6.4612[−1]	3.5028[−1]
$2s^22p^43s\ ^2D^e$–$2s^22p^43p\ ^2D^o$	2.0211[−5]	2.2550[−4]

[a] $a[\pm b]\equiv a\times 10^{\pm b}$.

TABLE V. Collision strengths for the electron excitation of atomic fluorine. The digits in brackets are the powers of 10 by which the preceding number is multiplied.

Transition	Collision strength									
i-*f*	1.20	1.40	1.60	1.80	2.00	2.20	2.40	2.60	2.80	3.00
1-2	2.473[−1]	2.479[−1]	2.167[−1]	1.993[−1]	1.849[−1]	1.648[−1]	1.488[−1]	1.356[−1]	1.226[−1]	1.096[−1]
1-3	3.977[−1]	6.277[−1]	9.063[−1]	1.155	1.272	1.414	1.550	1.668	1.796	1.898
1-4	6.529[−2]	8.405[−2]	9.914[−2]	9.533[−2]	8.770[−2]	7.610[−2]	6.454[−2]	5.721[−2]	4.709[−2]	4.250[−2]
1-5	6.860[−2]	1.284[−1]	1.364[−1]	1.262[−1]	1.103[−1]	9.424[−2]	7.851[−2]	6.835[−2]	5.999[−2]	5.205[−2]
1-6	1.078[−1]	1.828[−1]	2.145[−1]	2.231[−1]	2.126[−1]	2.060[−1]	2.024[−1]	2.003[−1]	2.033[−1]	2.011[−1]
1-7	1.062[−2]	2.054[−2]	2.845[−2]	3.117[−2]	3.095[−2]	2.967[−2]	2.829[−2]	2.740[−2]	2.698[−2]	2.579[−2]
1-8	2.242[−2]	4.740[−2]	4.212[−2]	3.189[−2]	2.487[−2]	1.929[−2]	1.512[−2]	1.223[−2]	1.061[−2]	8.688[−3]
1-9	3.548[−1]	6.023[−1]	7.561[−1]	8.665[−1]	9.615[−1]	1.038	1.039	1.128	1.126	1.131
1-10	3.797[−2]	2.762[−1]	6.112[−1]	1.548	6.155[−1]	6.306[−1]	6.691[−1]	7.146[−1]	7.525[−1]	7.919[−1]
1-11	2.403[−2]	5.461[−2]	6.330[−2]	5.292[−2]	4.155[−2]	3.180[−2]	2.459[−2]	1.984[−2]	1.564[−2]	1.320[−2]
2-3	9.650	8.464	4.176	2.292	1.481	1.085	9.014[−1]	7.813[−1]	7.122[−1]	6.989[−1]
2-4	4.291[+1]	9.230[+1]	1.382[+2]	1.773[+2]	2.106[+2]	2.391[+2]	2.641[+2]	2.857[+2]	3.053[+2]	3.228[+2]
2-5	5.255[+1]	1.644[+2]	2.413[+2]	3.016[+2]	3.516[+2]	3.935[+2]	4.301[+2]	4.620[+2]	4.901[+2]	5.164[+2]
2-6	4.382	4.541	2.354	1.356	8.674[−1]	6.294[−1]	4.933[−1]	4.072[−1]	3.688[−1]	3.134[−1]
2-7	7.883[−1]	7.635[−1]	4.440[−1]	2.574[−1]	1.638[−1]	1.166[−1]	8.909[−2]	7.161[−2]	6.538[−2]	5.294[−2]
2-8	7.486	2.897[+1]	4.402[+1]	5.503[+1]	6.404[+1]	7.161[+1]	7.820[+1]	8.391[+1]	8.901[+1]	9.366[+1]
2-9	2.328	2.521	1.241	6.985[−1]	4.462[−1]	3.289[−1]	2.643[−1]	2.42[−1]	2.016[−1]	1.764[−1]
2-10	2.035[−1]	1.550	1.420	1.666	1.869	2.056	2.142	2.276	2.255	2.323
2-11	7.188	2.754[+1]	3.563[+1]	3.874[+1]	4.007[+1]	4.051[+1]	4.050[+1]	4.033[+1]	3.981[+1]	3.953[+1]
3-4	2.556	3.662	1.793	9.326[−1]	5.683[−1]	3.948[−1]	3.093[−1]	2.551[−1]	2.195[−1]	1.951[−1]
3-5	6.112	5.663	2.571	1.373	8.538[−1]	6.048[−1]	4.739[−1]	3.918[−1]	3.378[−1]	2.946[−1]
3-6	2.709[+1]	9.423[+1]	1.395[+2]	1.728[+2]	1.995[+2]	2.215[+2]	2.406[+2]	2.567[+2]	2.715[+2]	2.843[+2]
3.7	4.335	1.649[+1]	2.512[+1]	3.139[+1]	3.646[+1]	4.066[+1]	4.428[+1]	4.737[+1]	5.018[+1]	5.265[+1]
3-8	1.062	1.067	4.973[−1]	2.665[−1]	1.629[−1]	1.119[−1]	8.449[−2]	6.833[−2]	5.477[−2]	4.695[−2]
3-9	1.212[+1]	4.771[+1]	7.310[+1]	9.211[+1]	1.074[+2]	1.200[+2]	1.309[+2]	1.404[+2]	1.487[+2]	1.564[+2]
3-10	2.313[−1]	1.072	1.669	1.052	1.285	1.311	1.291	1.266	1.463	1.395
3-11	1.912	1.906	1.008	5.496[−1]	3.679[−1]	2.722[−1]	2.116[−1]	1.706[−1]	1.311[−1]	1.119[−1]
4-5	4.887[+1]	7.768[+1]	9.453[+1]	1.022[+2]	1.074[+2]	1.128[+2]	1.185[+2]	1.266[+2]	1.332[+2]	1.424[+2]
4-6	1.891	3.545	1.930	1.035	6.423[−1]	4.615[−1]	3.561[−1]	3.112[−1]	2.494[−1]	2.280[−1]
4-7	5.793[−1]	5.289[−1]	1.642[−1]	8.685[−2]	5.564[−2]	4.421[−2]	3.616[−2]	3.561[−2]	2.778[−2]	2.737[−2]
4-8	2.606	2.984	2.739	2.848	2.883	2.887	2.864	2.845	2.795	2.749
4-9	4.458	6.674	3.579	2.070	1.419	1.145	9.595[−1]	9.079[−1]	7.551[−1]	7.514[−1]
4-10	5.911[−2]	1.370	1.408[−1]	1.687[−1]	1.729[−1]	1.708[−1]	1.644[−1]	1.582[−1]	1.464[−1]	1.359[−1]
4-11	3.916[+1]	2.957[+2]	5.216[+2]	6.987[+2]	8.421[+2]	9.626[+2]	1.066[+3]	1.156[+3]	1.236[+3]	1.307[+3]
5-6	1.128[+1]	1.460[+1]	7.854	4.503	2.948	2.254	1.822	1.684	1.384	1.322
5-7	8.315[−1]	1.905	1.16	7.082[−1]	4.862[−1]	3.724[−1]	2.920[−1]	2.565[−1]	1.987[−1]	1.806[−1]
5-8	3.682[+1]	4.402[+1]	4.817[+1]	4.967[+1]	5.011[+1]	5.033[+1]	5.035[+1]	5.045[+1]	5.007[+1]	5.009[+1]
5-9	2.253	3.267	1.982	1.093	6.728[−1]	4.718[−1]	3.541[−1]	3.006[−1]	2.332[−1]	2.062[−1]
5-10	2.332[−2]	1.208	2.187[−1]	2.631[−1]	2.530[−1]	2.444[−1]	2.244[−1]	2.195[−1]	1.880[−1]	1.814[−1]
5-11	2.731[+1]	1.660[+2]	2.610[+2]	3.252[+2]	3.742[+2]	4.143[+2]	4.478[+2]	4.775[+2]	5.028[+2]	5.270[+2]
6-7	1.811[+1]	2.226[+1]	2.531[+1]	2.615[+1]	2.626[+1]	2.625[+1]	2.612[+1]	2.607[+1]	2.577[+1]	2.574[+1]

TABLE V. (*Continued.*)

Transition	Collision strength									
i-*f*	1.20	1.40	1.60	1.80	2.00	2.20	2.40	2.60	2.80	3.00
6-8	1.026	1.820	1.151	7.372[−1]	5.031[−1]	3.832[−1]	2.981[−1]	2.588[−1]	2.054[−1]	1.863[−1]
6-9	3.484[+1]	4.663[+1]	5.268[+1]	5.503[+1]	5.669[+1]	5.879[+1]	6.122[+1]	6.428[+1]	6.776[+1]	7.176[+1]
6-10	2.357[−1]	1.289	7.846[−1]	7.088[−1]	7.617[−1]	7.833[−1]	7.934[−1]	8.077[−1]	8.322[−1]	8.397[−1]
6-11	2.726	5.790	3.257	1.632	9.492[−1]	6.199[−1]	4.310[−1]	3.295[−1]	2.387[−1]	1.987[−1]
7-8	1.548	2.169	1.142	6.232[−1]	4.023[−1]	3.085[−1]	2.519[−1]	2.346[−1]	1.976[−1]	1.906[−1]
7-9	1.124	1.339	1.678	1.844	1.851	1.820	1.771	1.734	1.691	1.661
7-10	2.013[−3]	1.703[−2]	1.013[−2]	8.315[−3]	8.427[−3]	8.818[−3]	9.070[−3]	9.354[−3]	9.824[−3]	9.643[−3]
7-11	2.863[−1]	7.987[−1]	3.827[−1]	1.632[−1]	8.611[−2]	5.390[−2]	3.620[−2]	2.844[−2]	1.955[−2]	1.547[−2]
8-9	3.851[−1]	7.429[−1]	2.386[−1]	1.050[−1]	5.721[−2]	3.881[−2]	2.867[−2]	2.562[−2]	1.959[−2]	1.834[−2]
8-10	9.678[−4]	6.578[−2]	6.216[−3]	9.000[−3]	1.125[−2]	1.232[−2]	1.316[−2]	1.375[−2]	1.273[−2]	1.297[−2]
8-11	8.473	3.434	3.246	2.913	2.636	2.396	2.187	2.019	1.853	1.727
9-10	2.939	9.585	1.143[+1]	1.246[+1]	1.328[+1]	1.401[+1]	1.472[+1]	1.538[+1]	1.595[+1]	1.650[+1]
9-11	3.232	6.213	3.129	1.615	9.555[−1]	6.288[−1]	4.432[−1]	3.362[−1]	2.568[−1]	2.067[−1]
10-11	3.956[−2]	2.238	1.653[−1]	1.545[−1]	1.249[−1]	1.054[−1]	8.741[−2]	7.985[−2]	6.071[−2]	5.588[−2]

B. Collision strength

The collision strengths for the electron-impact excitation of the fluorine atom are calculated for all the transitions involving the lowest 11 target states in a wide electron-energy range from the first excitation threshold to 3.0 Ry. In the region below the highest excitation threshold a fine-energy mesh is used to delineate any res-

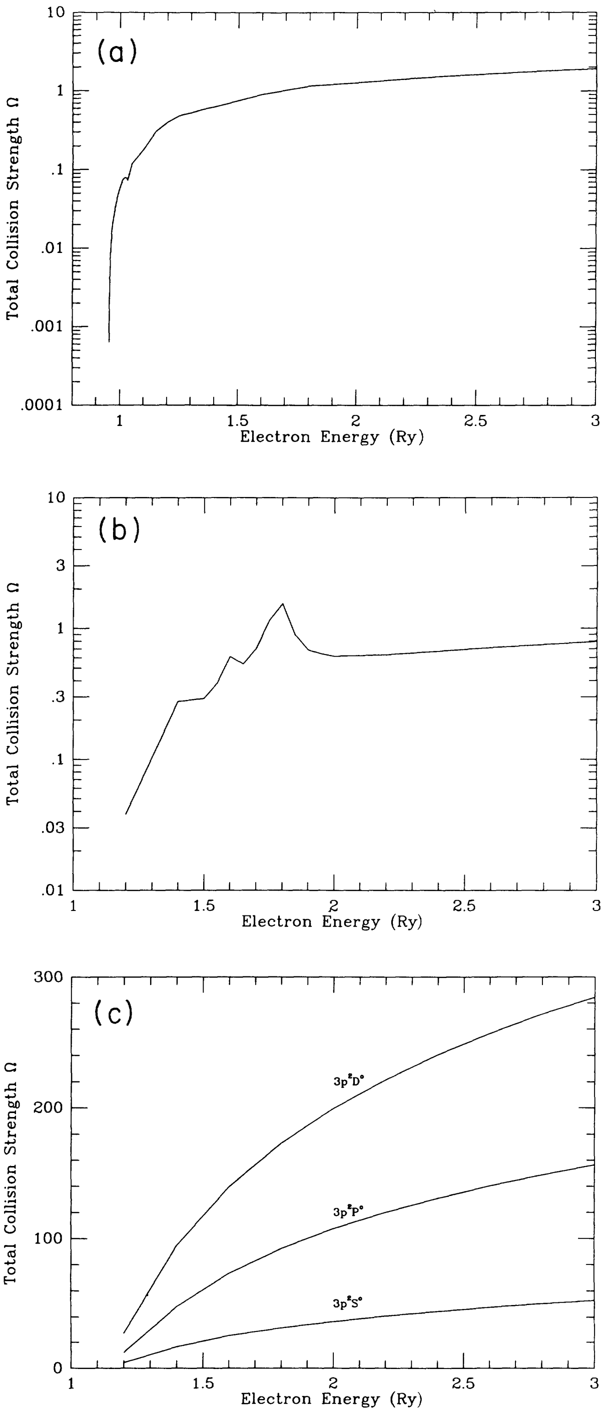

FIG. 1. Electron excitation collision strengths for the optically allowed transitions: (a) $2s^22p^5\,{}^2P^o$–$2s^22p^43s\,{}^2P$; (b) $2s^22p^5\,{}^2P^o$–$2s^22p^43s\,{}^2D$; and (c) $2s^22p^43s\,{}^2P$–$2s^22p^43p\,{}^2D^o$, ${}^2P^o$, ${}^2S^o$ in F I.

onance structure. Above the highest threshold included in the present calculation, the collision strengths are obtained at larger energy intervals. The standard full exchange R-matrix [10] method is used to calculate collision strengths for all the transitions in the partial-wave region with total angular momentum $L \leq 12$. The contribution of the partial waves with total angular momentum $13 \leq L \leq 40$ is calculated using the no-exchange program. In case of dipole-allowed transitions the higher ($L \geq 41$) partial-wave contribution is determined by applying the Burgess sum rule. The results seem to be completely converged.

Let us now comment on the contribution of the higher ($L > 12$) partial waves to the total collision strengths. In the case of the dipole-allowed transitions, this contribution is negligible (less than 1.5%) below the 1.4-Ry incident electron energy. However, the contribution of higher partial waves increases with incident energy and dominates the total collision strengths at the maximum energy (3.0 Ry) considered here. For all the dipole-allowed transitions the higher-partial-wave contribution to the total collision strength varies from 54% to 79% at this energy, except for the $2s^2 2p^5\,{}^2P^o$–$2s^2 2p^4 3s\,{}^2D$ transition, where this contribution is less than 2%. It should be noted that the application of the Burgess sum rule just after the total angular momentum $L = 12$, without using the no-exchange approximation for $13 \geq L \leq 40$, would result in an overestimation of the total collision strength by an amount of from 3% to 8% for most transitions. This overestimation of collision strengths is more than 30% for the dipole-allowed transition from the $3p\,{}^2P^o$ to $3s\,{}^2D$ state. However, the collision strengths for the transitions from the $3p\,{}^4P^o$ and $3p\,{}^4D^o$ states to the $3d\,{}^4D^e$ state are *underestimated* by about 18% and 6.6%, respectively.

For the dipole-forbidden transitions, the contribution of the higher ($L > 12$) partial waves varies from negligible to about 60% at the maximum incident electron energy used in the present calculation. The collision strengths for the $3p\,{}^4P^o$–$3p\,{}^4D^o$, $3p\,{}^2D^o$–$3p\,{}^2S^o$, $3p\,{}^4P^o$–$3p\,{}^4S^o$, $3p\,{}^4D^o$–$3p\,{}^4S^o$, $3p\,{}^2D^o$–$3p\,{}^2P^o$, $3s\,{}^4P^e$–$3d\,{}^4D^e$, and $3p\,{}^4S^o$–$3d\,{}^4D^e$ transitions increase by more than 10% by the inclusion of the contributions from $L > 12$ obtained using the no-exchange approximation. It therefore is very important to carry out calculations in the higher-partial-wave region, especially for the forbidden transitions.

The total collision strengths as a function of incident electron energy (in rydbergs) are plotted for some of the transitions in Figs. 1–3. The results are also presented in tabular form (Table V) for all the transitions above the highest threshold included in the present calculation.

Figures 1(a)–1(c) show the collision strengths plotted for the dipole-allowed transitions, $2p^5\,{}^2P^o$–$2p^4 3s\,{}^2P$, $2p^5\,{}^2P^o$–$2p^4 3s\,{}^2D$, and $2p^4 3s\,{}^2P$–$2p^4 3p\,{}^2D^o$, ${}^2P^o$, ${}^2S^o$. These are characterized by an increase in the collision strengths with electron energy. However, the collision strength for the transition from ground state $2s^2 2p^5\,{}^2P^o$ to excited state $2s^2 2p^4 3s\,{}^2D$ shows a structure between 1.4- and 1.9-Ry energies. The excitation of the $3s\,{}^2P^e$ state to the $3p\,{}^2S^o$, ${}^2P^o$, and $3p\,{}^2D^o$ states is displayed in Fig. 1(c). Figures 2(a)–2(c) show the collision strengths as a function of electron energy for the excitation of the metastable state $2s^2 2p^4 3s\,{}^4P^e$ to the $2p^4 3s\,{}^2P$, $2p^4 3p\,{}^4D^o$, ${}^4P^o$, ${}^4S^o$, and $2p^4 3p\,{}^2D^o$, ${}^2P^o$, ${}^2S^o$ target states. The cross sections for the dipole-allowed transitions from the metastable state ${}^4P$ are very large [Fig. 2(b)]. Figures 3(a)–3(d)

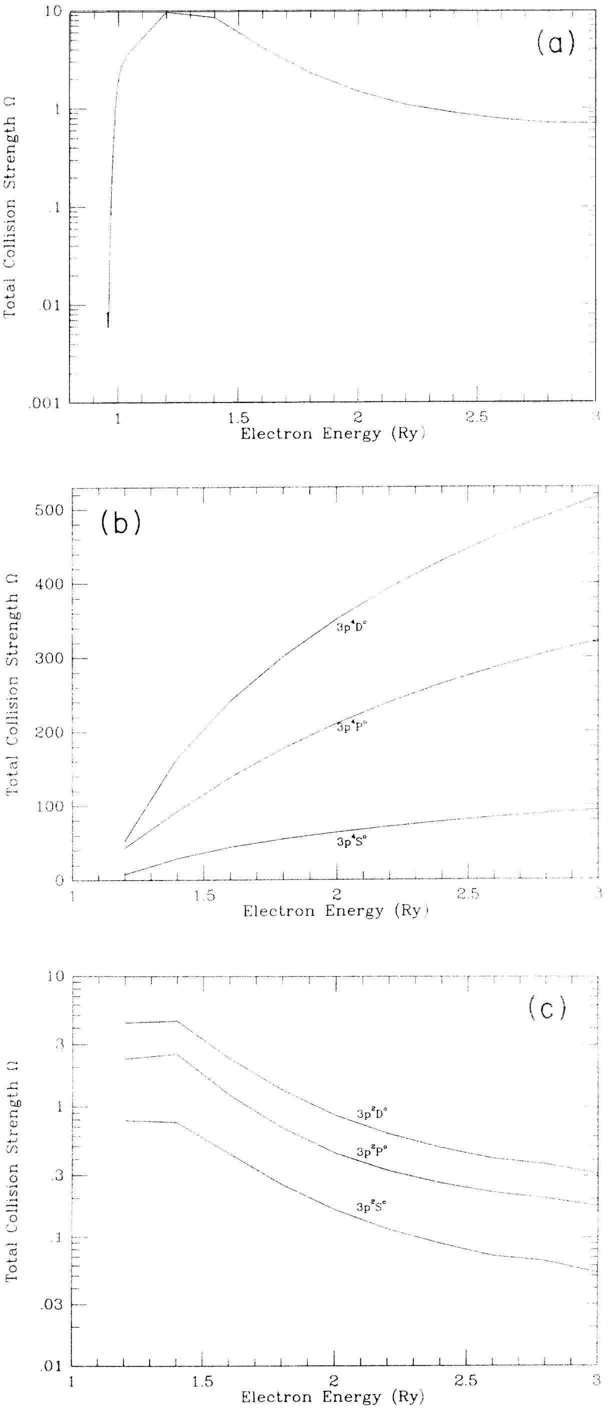

FIG. 2. Collision strengths for the electron excitation of metastable-state $2s^2 2p^4 3s\,{}^4P$ to the (a) $2s^2 2p^4 3s\,{}^2P$; (b) $2s^2 2p^4 3p\,{}^4D^o$, ${}^4P^o$, ${}^4S^o$; and (c) $2s^2 2p^4 3p\,{}^2D^o$, ${}^2P^o$, ${}^2S^o$ states of F I.

display collision strengths for some of the forbidden transitions. The shown transitions are from the ground state ${}^2P^o$ to $3s\,{}^4P$, $3p\,{}^4D^o$, $3p\,{}^2S^o$ and from the $3s\,{}^2P$ to the $3p\,{}^4P^o$, ${}^4D^o$ states. The collision strengths for these transitions, generally, first increase sharply and then decrease slowly with energy.

It is interesting to note from Table V that total collision strengths for most of the transitions between excited states reported here for neutral fluorine are very large compared to what one gets for the ions [8]. The large collision strengths for these transitions suggest that the higher excited states have substantial population in neutral systems.

IV. CONCLUSION

The absorption oscillator strengths and collision strengths for the excitation of the fluorine atom are calculated with the lowest 11 target states retained in the calculation. The initial- and final-state collision wave functions are represented consistently in terms of the R-matrix basis functions. The calculated and observed target-state energies show good agreement. However, the observed values of the excitation energies are used in the scattering calculation. The use of the no-exchange program for the calculation above total angular momentum $L=12$ and up to $L=40$ provides an efficient way of getting converged results for almost all the transitions. This is particularly true of some dipole-forbidden transitions for which a significant contribution comes from this partial-wave region. For dipole-allowed transitions the higher-partial-wave contribution is determined by using Burgess sum rule. However, it is found that collision strengths have already been mostly converged and that the higher $(L>40)$ partial-wave contribution is very small.

It is seen that the collision strengths for many transitions are larger for neutral fluorine compared to F-like ions [8]. It points to a comparatively higher population of excited states in neutral atoms than the population of these states in the positive ions. The present results for the collision strengths are expected to be of high accuracy in the energy range considered. We notice that to obtain accurate results above this energy one has to include

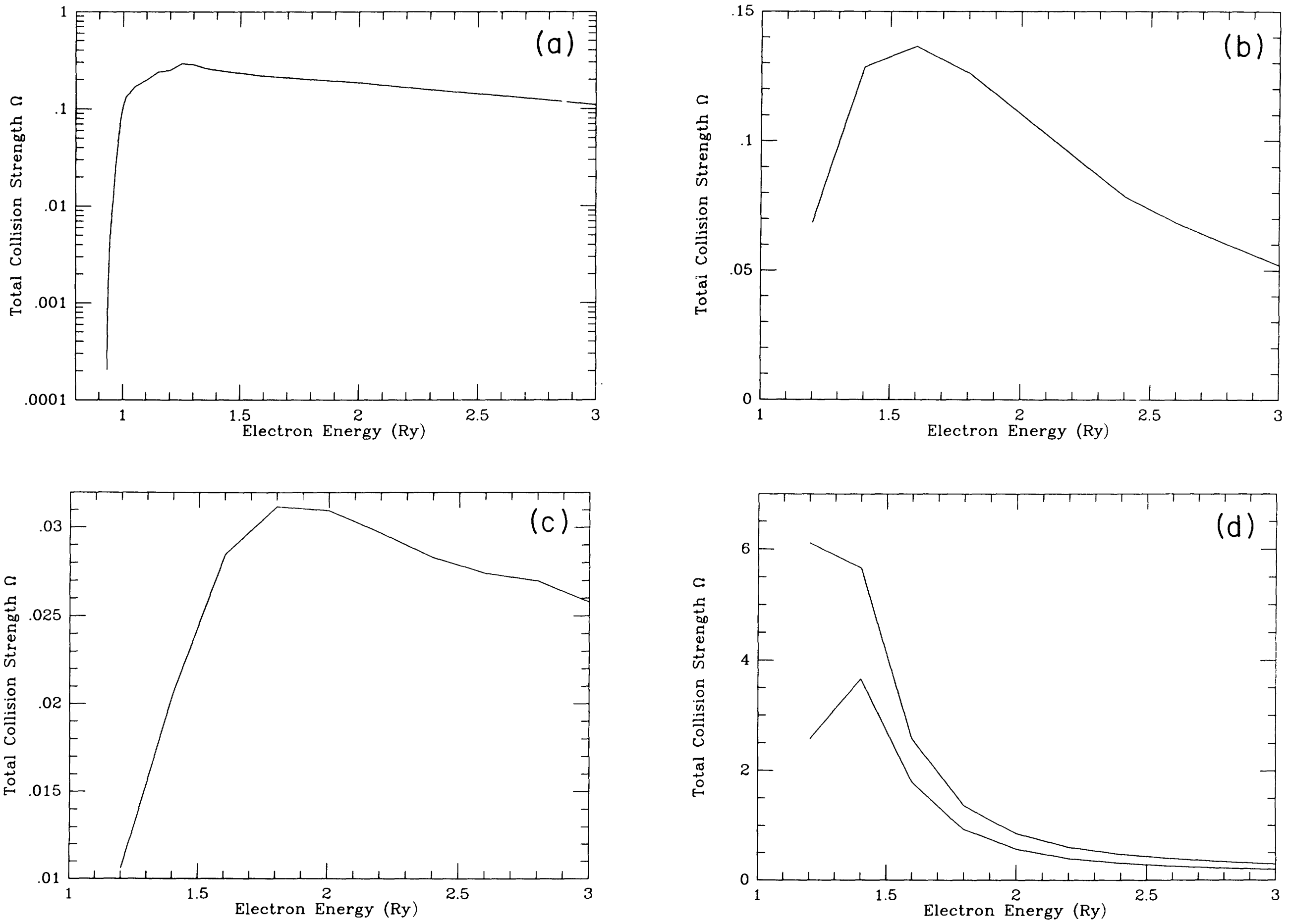

FIG. 3. Electron excitation collision strengths for the forbidden transitions: (a) $2s^22p^5\,{}^2P^o$–$2s^22p^43s\,{}^4P$; (b) $2s^22p^5\,{}^2P^o$–$2s^22p^43p\,{}^4D^o$; (c) $2s^22p^5\,{}^2P^o$–$2s^22p^43p\,{}^2S^o$; and (d) $2s^22p^43s\,{}^2P$–$2s^22p^43p\,{}^4D^o$, $4P^o$ in F I.

all the target states spanning that energy region. Nevertheless, the present results can be used for a higher energy region than that reported here with a loss of accuracy of not more than 20%. The results reported here will mainly be affected by any resonance structure associated with the new channels that become open at higher energies. We have also calculated the cross sections for the elastic scattering of electrons from the ground and excited states of neutral fluorine, which will be reported elsewhere.

ACKNOWLEDGMENTS

The calculations were performed on the CRAY-YMP/C98 computer at NASA Center for Computation Science, Goddard Space Flight Center, and analyzed on the VAX-6250. We would like to thank Alan Silver for providing extra computer time on Cray. One of us (K.S.B.) acknowledges financial support from the National Research Council. This work was funded by NASA under Grant No. RTOP 188-38-53-14.

---

[1] K. Liden, Ark. Phys. **1**, 229 (1949).
[2] R. E. Huffman, J. C. Larrabee, and Y. Tanaka, J. Chem. Phys. **47**, 856 (1967).
[3] H. P. Palenius, Ark. Phys. **39**, 425 (1969).
[4] H. P. Palenius, R. E. Huffman, J. C. Larrabee, and Y. Tanaka, J. Opt. Soc. Am. **68**, 1564 (1978).
[5] K. Ono, T. Oomori, Y. Ueda, K. Sato, K. Toi, T. Watari, I. Ogawa, K. Kawahato, R. Ando, Y. Kawasumi, N. Noda, and S. Tanahadi, Phys. Rev. A **34**, 1328 (1986).
[6] M. C. B. Ashley and A. R. Hyland, Astrophys. J. **331**, 532 (1988).
[7] S. Suckewer, R. Fonck, and E. Hinnoy, Phys. Rev. A **21**, 972 (1980).
[8] M. Mohan and A. Hibbert, Phys. Scr. **44**, 158 (1991).
[9] P. G. Burke and W. D. Robb, Adv. At. Mol. Phys. **11**, 143 (1975).
[10] K. A. Berrington, P. G. Burke, M. Le Dourneuf, W. D. Robb, K. T. Taylor, and Vo Ky Lan, Comput. Phys. Commun. **14**, 367 (1978).
[11] V. M. Burke, P. G. Burke, and N. S. Scott, Comput. Phys. Commun. **69**, 76 (1992).
[12] A. Burgess, J. Phys. B **7**, 287 (1974).
[13] E. Clementi and C. Roetti, At. Data Nucl. Data Tables **14**, 177 (1974).
[14] A. Hibbert, Comput. Phys. Commun. **9**, 141 (1975).
[15] W. L. Wiese and G. A. Martin, *Wavelengths and Transition Probabilities for Atoms and Atomic Ions,* Natl. Bur. Stand. Ref. Data Ser., Natl. Bur. Stand. (U.S.) Circ. No. 68 (U.S. GPO, Washington, D.C., 1980), Pt. II, p. 377.
[16] K. A. Berrington, V. M. Burke, P. G. Burke, and S. Sciala, J. Phys. B **22**, 665 (1978).
[17] J. P. Croskery, N. S. Scott, K. L. Bell, and K. A. Berrington, Comput. Phys. Commun. **27**, 385 (1982).
[18] K. A. Berrington, P. G. Burke, K. Butler, M. J. Seaton, P. J. Storey, K. T. Taylor, and Yu Yan, J. Phys. B **20**, 6379 (1987).